ISSCR

PBX1-directed stem cell transcriptional program drives tumor progression in myeloproliferative neoplasm

Sharon Muggeo,[1,2,10,14] Laura Crisafulli,[1,2,14] Paolo Uva,[3,11] Elena Fontana,[1,2] Marta Ubezio,[4] Emanuela Morenghi,[5] Federico Simone Colombo,[6,12] Rosita Rigoni,[1,2] Clelia Peano,[1,7,13] Paolo Vezzoni,[1,2] Matteo Giovanni Della Porta,[4,8] Anna Villa,[1,9] and Francesca Ficara[1,2,*]

[1]UOS Milan Unit, Istituto di Ricerca Genetica e Biomedica (IRGB), CNR, Milan, Italy
[2]Human Genome and Biomedical Technologies Unit, IRCCS Humanitas Research Hospital, via Manzoni 56, Rozzano, Milan 20089, Italy
[3]CRS4, Science and Technology Park Polaris, Pula (CA), Italy
[4]Department of Oncology and Hematology, IRCCS Humanitas Research Hospital, via Manzoni 56, Rozzano, 20089 Milan, Italy
[5]Biostatistics Unit, IRCCS Humanitas Research Hospital, via Manzoni 56, Rozzano, Milan, Italy
[6]Flow Cytometry Core, IRCCS Humanitas Research Hospital, via Manzoni 56, Rozzano, 20089 Milan, Italy
[7]Genomic Unit, IRCCS Humanitas Research Hospital, via Manzoni 56, Rozzano, 20089 Milan, Italy
[8]Department of Biomedical Sciences, Humanitas University, Via Rita Levi Montalcini 4, Pieve Emanuele, 20090 Milan, Italy
[9]San Raffaele Telethon Institute for Gene Therapy (SR-TIGET), IRCCS San Raffaele Scientific Institute, Milan, Italy
[10]Present address: Stem Cell and Neurogenesis Unit, Division of Neuroscience, San Raffaele Scientific Institute, Milan, Italy
[11]Present address: IRCCS G. Gaslini, 16147 Genoa, Italy
[12]Present address: Servizio di Citofluorimetria, Fondazione IRCCS Ca' Granda Ospedale Maggiore Policlinico, Milan, Italy
[13]Present address: Human Technopole, Via Rita Levi Montalcini 1, Milan, Italy
[14]These authors contributed equally
*Correspondence: francesca.ficara@humanitasresearch.it
https://doi.org/10.1016/j.stemcr.2021.09.016

SUMMARY

PBX1 regulates the balance between self-renewal and differentiation of hematopoietic stem cells and maintains proto-oncogenic transcriptional pathways in early progenitors. Its increased expression was found in myeloproliferative neoplasm (MPN) patients bearing the $JAK2^{V617F}$ mutation. To investigate if PBX1 contributes to MPN, and to explore its potential as therapeutic target, we generated the JP mouse strain, in which the human $JAK2$ mutation is induced in the absence of PBX1. Typical MPN features, such as thrombocythemia and granulocytosis, did not develop without PBX1, while erythrocytosis, initially displayed by JP mice, gradually resolved over time; splenic myeloid metaplasia and *in vitro* cytokine independent growth were absent upon PBX1 inactivation. The aberrant transcriptome in stem/progenitor cells from the MPN model was reverted by the absence of PBX1, demonstrating that PBX1 controls part of the molecular pathways deregulated by the JAK2^{V617F} mutation. Modulation of the PBX1-driven transcriptional program might represent a novel therapeutic approach.

INTRODUCTION

Myeloproliferative neoplasms are heterogeneous diseases in which platelets and/or mature blood cells of the myelo-erythroid lineage are produced in large excess (Tefferi, 2016) and that can ultimately evolve into acute leukemia. The three main MPN subtypes are polycythemia vera (PV), essential thrombocythemia (ET), and primary myelofibrosis (PMF), often characterized by the somatic V617F mutation in the JAK2 tyrosine kinase, which renders it constitutively active irrespective of cytokine stimulation. $JAK2^{V617F}$ is considered a phenotypic driver mutation (Nangalia and Green, 2017), although it is not sufficient to explain the heterogeneity of these diseases. Despite MPN being due to hyperproduction of mature cells, $JAK2^{V617F}$ is present in patients' hematopoietic stem cells (HSCs), suggesting that they are targets of the initiating genetic lesion (Mead and Mullally, 2017).

PBX1 is a homeodomain transcription factor that binds DNA as a complex with HOX and MEIS/PREP proteins (Longobardi et al., 2014; Moens and Selleri, 2006), and that

is involved in chromosomal translocations leading to pediatric pre-B acute lymphoblastic leukemia (Nourse et al., 1990). PBX1 is one of the key factors regulating the balance between self-renewal and differentiation in HSCs (Ficara et al., 2008). In addition, PBX1 acts in multipotent and common myeloid progenitors to preserve their pool by temporally restricting proliferation and myeloid differentiation, and to preserve lymphoid and erythroid potential (Ficara et al., 2013). Bioinformatics analysis of gene expression data and experimental evidence revealed that PBX1 maintains proto-oncogenic transcriptional pathways involved in solid tumors and in myelo-proliferative disorders (Ficara et al., 2013; Jung et al., 2016; Wei et al., 2018), conceivably by virtue of its role in inhibiting differentiation in multiple stages of the hematopoietic hierarchy. Indeed, *PBX1* copy number variation was found in a subset of MPN patients bearing $JAK2^{V617F}$ mutation (Rice et al., 2011), and PBX1 is overexpressed in cluster of differentiation (CD) 34^{+} cells from PV patients (Berkofsky-Fessler et al., 2010). Moreover, *Pbx1* is downregulated in murine Jak2-deficient hematopoietic stem and progenitor cells (HSPCs) (Akada et al., 2014), suggesting that it is part of

Table 1. Overlap between MPN and PBX1 signatures

Study	Sorted cells	MPN subgroup	Gene set size (DE IN MPN)		Common with PBX1 signature (IC DE)[a]	p-value
Rice et al., 2011	PB granulocytes	PV, ET, PMF	UP:	766	52 (6.8%)[b]	2.6×10^{-9}
			DOWN:	454	5 (1.1%)	n.s.
Rampal et al., 2014	PB granulocytes	PV, ET, PMF	UP:	1608	94 (5.8%)	2.5×10^{-12}
			DOWN:	1606	16 (1.0%)	n.s.
Berkofsky-Fessler et al., 2010	BM CD34+	PV	UP:	49	12 (24.5%)	6.7×10^{-9}
			DOWN:	243	9 (3.7%)	0.0027
Guglielmelli et al., 2007	PB CD34+	PMF	UP:	185	25 (13.5%)	6.2×10^{-11}
			DOWN:	211	12 (5.7%)	9.6×10^{-6}

The PBX1 signature and the lists of common genes are included in Tables S1 and S3, respectively. IC, inversely correlated. n.s., not significant.
[a]Overlap analysis refers to common and anti-correlated genes.
[b]Percentage values in brackets is calculated on the corresponding MPN DE values.

JAK2 signaling, and its overexpression in *JAK2*-mutant HSCs contributes to sustaining an MPN phenotype *in vivo* (Shepherd et al., 2018). Therefore, we reasoned that an aberrant expression of PBX1 or of its targets might contribute to the establishment or the maintenance of myeloid pre-leukemic clones. To test this hypothesis, we generated a new mouse model by crossing a *Pbx1*-conditional knockout (*Pbx1*-cKO) (Ficara et al., 2008) with a known *JAK2^{V617F}* MPN model (*JAK2^{V617F}*-conditional knockin [*JAK2*-cKI], developed by Li et al., 2010). In *JAK2*-cKI/*Pbx1*-cKO mice (hereafter JP for brevity), we can simultaneously activate the human *JAK2* mutation and delete *Pbx1* in the adult HSC compartment upon polyinosinic-polycytidylic acid (pIpC) administration.

We demonstrate that PBX1 plays a crucial role in MPN, since its absence modified the course of MPN: our model showed initial JAK2-dependent erythrocytosis that progressively disappeared after conditional PBX1 deletion, and the absence of other MPN-like symptoms. Therefore, PBX1 is essential for the maintenance of the malignant clone, rather than for initiating the disease. We also show that, despite the blood pathology in MPN being mediated by differentiated cells, transcriptional changes already occur at the level of early progenitors. RNA sequencing (RNA-seq) data confirmed that PBX1 in HSPCs controls part of the molecular pathways deregulated by the *JAK2^{V617F}* mutation.

RESULTS

### Pbx1 controls part of the MPN signature

We first interrogated the literature to find some *in silico* evidence of a possible involvement of PBX1 in human MPN. We retrieved a human MPN expression profile from four previously published studies (Berkofsky-Fessler et al., 2010; Guglielmelli et al., 2007; Rampal et al., 2014; Rice et al., 2011), in which data have been obtained either from granulocytes of several PV, PMF, or ET patients, or from CD34+ cells of PV or PMF patients. There is a considerable overlap between the two studies with similar disease subgroup and cell sources (Figures S1A and S1B and Table 1). A PBX1-dependent transcriptional program was obtained from our previously published profiles of *Pbx1*-cKO HSCs and progenitors (Table S1). When we compared the PBX1 and each MPN signature, we found that a significant proportion of the genes downregulated in the absence of PBX1 are upregulated in MPN patients (Table 1, up to 24.5% overlap). Similarly, a significant proportion of the genes upregulated in the absence of PBX1 are downregulated in CD34+ cells of PV and PMF patients. This is in accordance with the hypothesis that PBX1, directly or indirectly, may control part of the MPN signature. In addition, in the bone marrow (BM) CD34− fraction of five *JAK2^{V617F}* patients analyzed, we found a tendency to a higher expression of PBX1 compared with healthy donors, despite PBX1 being a stem cell transcription factor that is expected to be expressed mainly in the CD34+ fraction (Figure S1C).

These data provided a strong rationale for asking if MPN course might be modified by acting on PBX1 or on its molecular signature.

PBX1 expression in *JAK2^{V617F}* HSCs is necessary to sustain MPN

To explore the role of PBX1 in MPN, we undertook a classic genetic approach, by crossing a previously described *JAK2^{V617F}* inducible knockin MPN model (Li et al., 2010) with a *Pbx1*-cKO mouse (Ficara et al., 2008). In the resulting
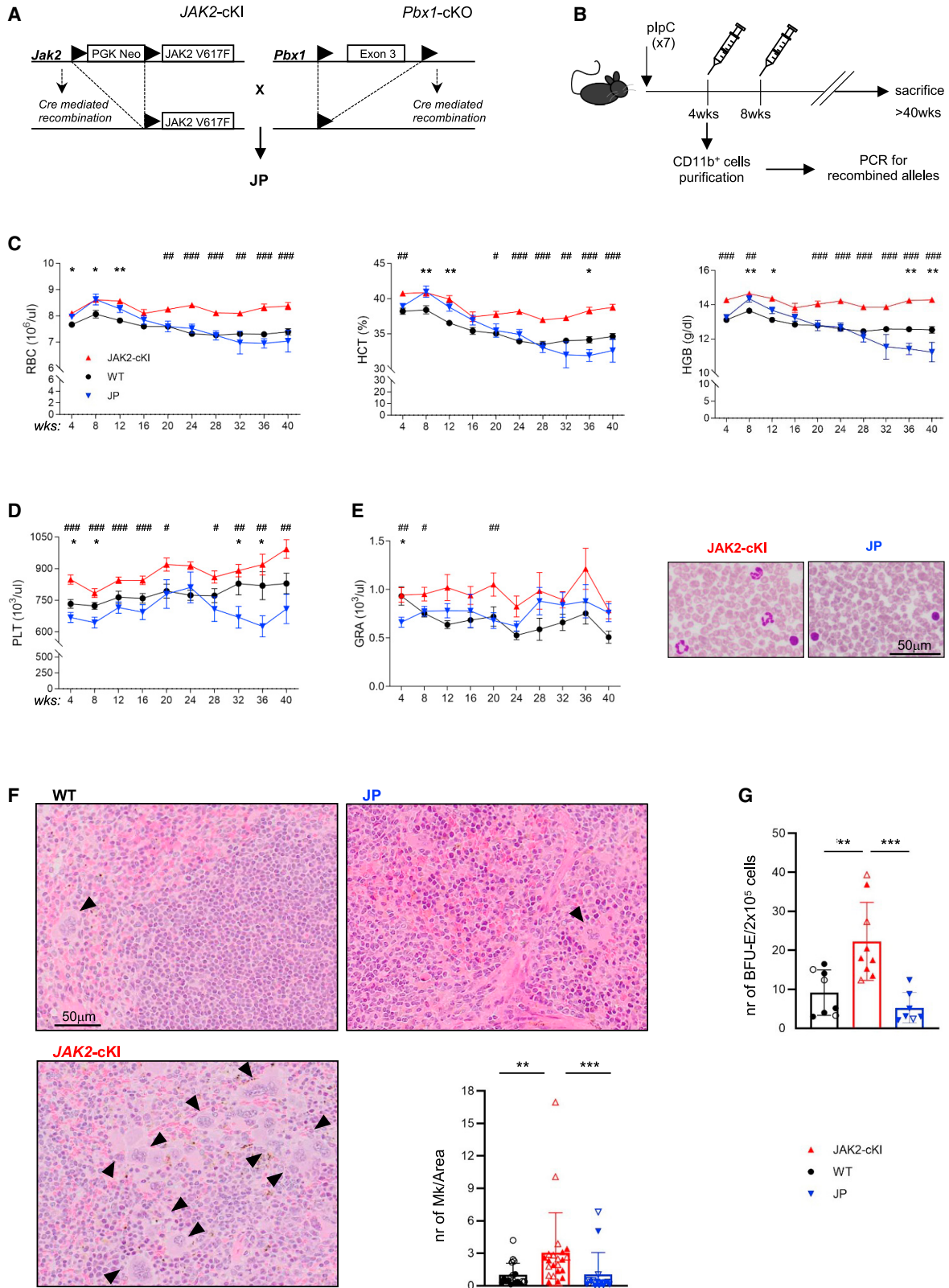
(legend on next page)

double-mutant JP mouse, the activation of the MPN-driver human heterozygous $JAK2^{V617F}$ mutation and PBX1 deletion are induced simultaneously by repeated pIpC injections (Figures 1A and 1B). Recombination was always verified at the first peripheral blood (PB) draw (and at necropsy on BM-derived colonies; see also Note S1 and Figure S2).

We followed the disease kinetics for several weeks in *JAK2*-cKI and in JP mice, by comparing their blood parameters with those of our cohort of wild-type (WT) and *Pbx1*-cKO control mice. Starting from 4 weeks after the last pIpC injection, PB was drawn at regular intervals and analyzed by hemocytometer, up to at least 40 weeks from Cre induction. *JAK2*-cKI mice developed a mild but significant erythrocytosis in both male and female mice, with increased hematocrit, hemoglobin (HGB), and red blood cell counts compared with WT mice, as expected (Figures 1C and S3A). In JP mice, a similar increase in all these parameters was noted up to 12 weeks after pIpC (Figure 1C), despite conditional inactivation of PBX1 alone leading to anemia (Figure S3B). At later time points, however, erythrocytosis was progressively less evident in JP mice, reaching at week 16–20 hematological parameters similar to those of WT mice (Figure 1C). HGB values were even lower than those of WT mice at the latest time points, raising some concern regarding possible development of a mild form of hypochromic anemia in the long run, as suggested by analyzing median corpuscular hemoglobin (MCH) and MCH concentration (MCHC) values (Figure S3C). JP platelet counts, on the other hand, were similar to or lower than those of WT mice throughout the observation time,

including the earliest time points (Figures 1D and S3D), suggesting a prominent role of Pbx1 in platelet development or production, as suggested by the thrombocythemia observed in *Pbx1*-cKO mice (Figure S3E). The increase in granulocyte counts was also rescued, starting from the first observation times (Figure 1E, left; a representative blood smear is shown on the right), but only up to week 24 and week 8 in male or female mice, respectively (Figure S3F), whereas at later time points the high variability in all experimental groups hampered further evaluations. Overall, the absence of PBX1 rescued the alteration of blood parameters in *JAK2*-cKI mice.

JAK2-cKI and all control mice survived throughout all the observation time, including *Pbx1*-cKO mice, despite their stem cell defect. Although features of MPN were abrogated in the absence of PBX1, some JP mice succumbed for unknown reasons, with signs of pancytopenia for some of them (Figure S4A). At necropsy, FACS analysis of BM and spleen showed that the proportion of lymphoid (CD19$^+$, CD4$^+$, CD8$^+$) and myeloid (CD11b$^+$) cells was similar in all mice (not shown). Histology data confirmed development of an MPN-like disease in *JAK2*-cKI mice, which displayed myeloid metaplasia in the spleen, indicated by the presence of megakaryocytic hyperplasia and of excess of myeloid cells (Figure 1F), but not in JP mice or in control animals (Figures 1F and S4B). Quantification of the splenic megakaryocytes revealed a complete normalization of this phenotype in the absence of PBX1 (Figure 1F). Finally, colony assays performed with BM cells derived from mice revealed that the *in vitro* EPO independent burst forming unit-erythroid (BFU-E) growth typical of MPN cells from

Figure 1. Generation and analysis of the JP mouse model

(A) Crossing of *Mx1Cre*$^+$.*JAK2*$^{+/V617F}$ (*JAK2*-cKI) with *Pbx1*$^{fl/fl}$ (*Pbx1*-cKO) mice generated the double-mutant JP model *Mx1Cre*$^+$. *JAK2*$^{+/V617F}$.*Pbx1*$^{fl/fl}$. Diagram on the left shows the *JAK2*^{V617F} knockin allele and the activated recombined allele after Cre-mediated excision of the PGK *Neo* cassette due to the presence of *LoxP* sites. On the right, *LoxP* sites surrounding exon 3 of *Pbx1* allow the allele recombination resulting in *Pbx1* inactivation.

(B) WT, *JAK2*-cKI, or JP mice, 4–6 weeks old, were administered with pIpC. Starting 4 weeks from last injection, PB was analyzed periodically. At the end of the monitoring period, animals were sacrificed to analyze BM and spleen. CD11b$^+$ cells were purified from PB at the first blood withdrawal.

(C–E) Time course analysis of blood parameters in *JAK2*-cKI, WT, and JP mice. Results from male and female mice were pooled, see Figure S3 for separate values. (C) Red blood cell (RBC) counts, hematocrit (HCT), and hemoglobin (HGB); (D) platelet (PLT) counts; (E) granulocyte (GRA) counts, with representative week 20 blood smear images on the right. Data are represented as mean ± SEM (n = 19–21 individual mice). For each plot, *wks* on x axis refers to weeks from the last pIpC injection. For each parameter, the entire trend of *JAK2*-cKI and WT mice is significantly different; p = 0.0001 in (C) and (E), p = 0.03 in (D) (these statistics are not shown within the graph for simplicity). Asterisk (*) and hash (#) symbols within the graphs indicate p values for each time point. Asterisk refers to the comparison between JP and WT mice, hash to the comparison between JP and *JAK2*-cKI mice. Images were acquired with an Olympus XC50 camera mounted on a BX51 microscope, using CellF Imaging software. Scale bar within the right panel refers to both images.

(F) Representative images of spleen histology (H&E staining) showing myeloid metaplasia with megakaryocytic hyperplasia in *JAK2*-cKI mice. Quantification of megakaryocytes (number of Mk/area) is represented in the scatterplot; n = 15–22 individual mice; Kruskal-Wallis test. Scale bar within the upper left panel refers to all three images.

(G) Scatterplot indicating the number of BFU-E generated from 2×10^5 total BM cells in the absence of EPO in the three mouse models; n = 8, 9, and 7 individual WT, *JAK2*-cKI, and JP mice, respectively; ordinary one-way ANOVA test. In (F) and (G), bars indicate mean ± SD. * and $^\#$, p < 0.05; ** and $^{\#\#}$, p < 0.01; *** and $^{\#\#\#}$, p < 0.001.
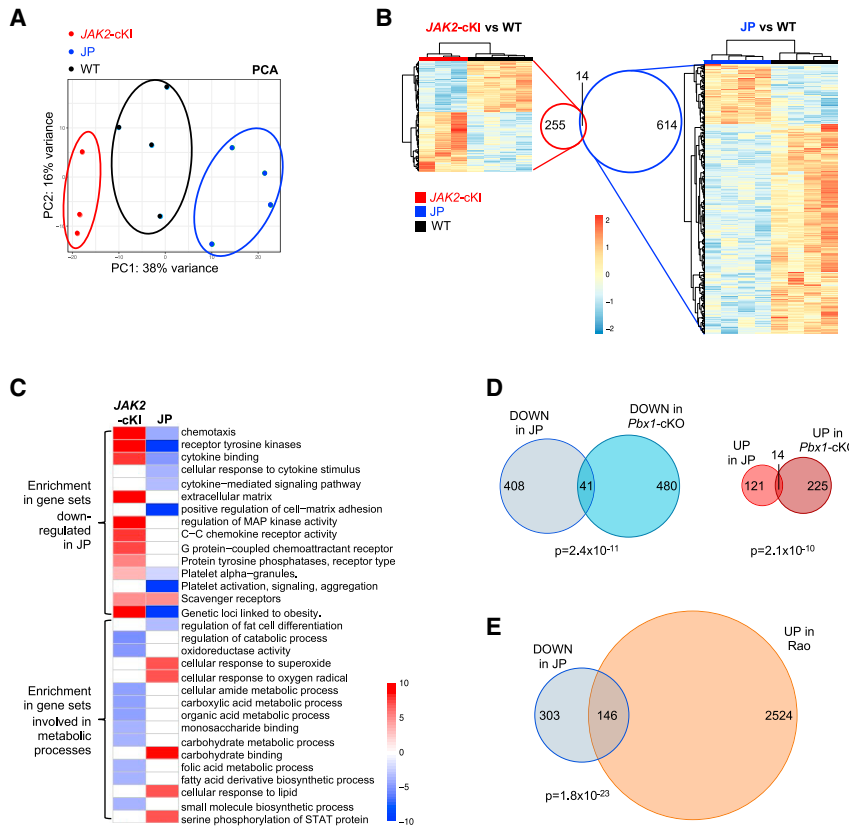
Figure 2. RNA-seq to discover molecular pathways deregulated in absence of PBX1

(A) PCA of *JAK2*-cKI, JP, and WT LKS (red, blue, and black, respectively).

(B) Hierarchical cluster dendrogram showing the relative expression of DE transcripts in *JAK2*-cKI LKS compared with WT (left) and in JP LKS compared with WT (right). Venn diagram shows the overlap of deregulated genes in the two analyses. The color scale represents *Z* score transformed signal intensity.

(C) Heatmap showing the enrichment score (minimum, −10; maximum, 10) from gene set enrichment analysis in the indicated categories for each gene set compared with WT.

(D) Venn diagrams showing overlaps among genes downregulated (left) and upregulated (right) in both JP and *Pbx1*-cKO HSPCs.

(E) Venn diagram showing overlap among genes downregulated in JP LKS and genes upregulated in MEP from VF mice, a transgenic MPN model with *Jak2^{V617F}* mutation described in Rao et al. (2019).

the *JAK2*-cKI mouse model (Li et al., 2010) was rescued in the absence of PBX1 (Figure 1G).

In conclusion, PBX1-dependant pathways control disease course for at least 40 weeks after the induction of the disease.

PBX1 controls molecular pathways deregulated by the *JAK2^{V617F}* mutation in HSPCs

To discover pathways deregulated by the *JAK2^{V617F}* mutation that are already affected by Pbx1 at the level of HSPCs, we performed RNA-seq on FACS-sorted Lineage⁻/cKit⁺/Sca1⁺ (LKS) cells from the BM of individual WT, *JAK2*-cKI, and JP mice several weeks after induction of the *JAK2* mutation and/or PBX1 deletion. Transcriptional data on *Pbx1*-cKO control HSPCs were already available (Ficara et al., 2008) and are included in Table S1. LKS were chosen since they are enriched for HSCs (Figure S4C, top panels), but they also include committed progenitors, thus comprising the cell population(s) that most likely sustain the disease long term; the proportion of LKS within the BM was similar in the three groups of mice, as well as the proportion of HSCs within LKS (Figure S4C, bottom).

Principal component analysis (PCA) shows that LKS from *JAK2*-cKI, WT, and JP mice cluster separately (Figure 2A), indicating intra-group homogeneity and good sample reso-

lution among the three conditions. Differential expression analysis revealed that 269 and 628 genes were differentially expressed (DE) at false discovery rate <0.05 in *JAK2*-cKI and in JP mice compared with WT, respectively (Figure 2B and Table S2). There was only a minimal overlap between the two gene sets (Figure 2B), indicating that the expression level of the vast majority of the genes DE in MPN-affected mice compared with WT was rescued by the absence of PBX1, since they were no longer DE in JP mice compared with WT. Of the 14 common genes, nine changed discordantly in the two gene sets: four were upregulated in *JAK2*-cKI but downregulated in JP mice, mostly involved in vesicular trafficking, and five were downregulated in *JAK2*-cKI but upregulated in JP mice (Table S2).

Genes downregulated in LKS from *JAK2*-cKI mice compared with WT were enriched for several metabolic processes (Figure 2C, bottom). A misregulation of genes involved in metabolism in megakaryocyte-erythrocyte progenitors (MEPs) has been described (Rao et al., 2019), and we here show that similar alterations are already present at the level of uncommitted cells in *JAK2*-cKI, but not in JP mice. Genes upregulated in LKS from *JAK2*-cKI mice compared with WT were enriched for several gene families and pathways involved in MPN pathogenesis, including receptor tyrosine kinases, extracellular matrix, cytokine
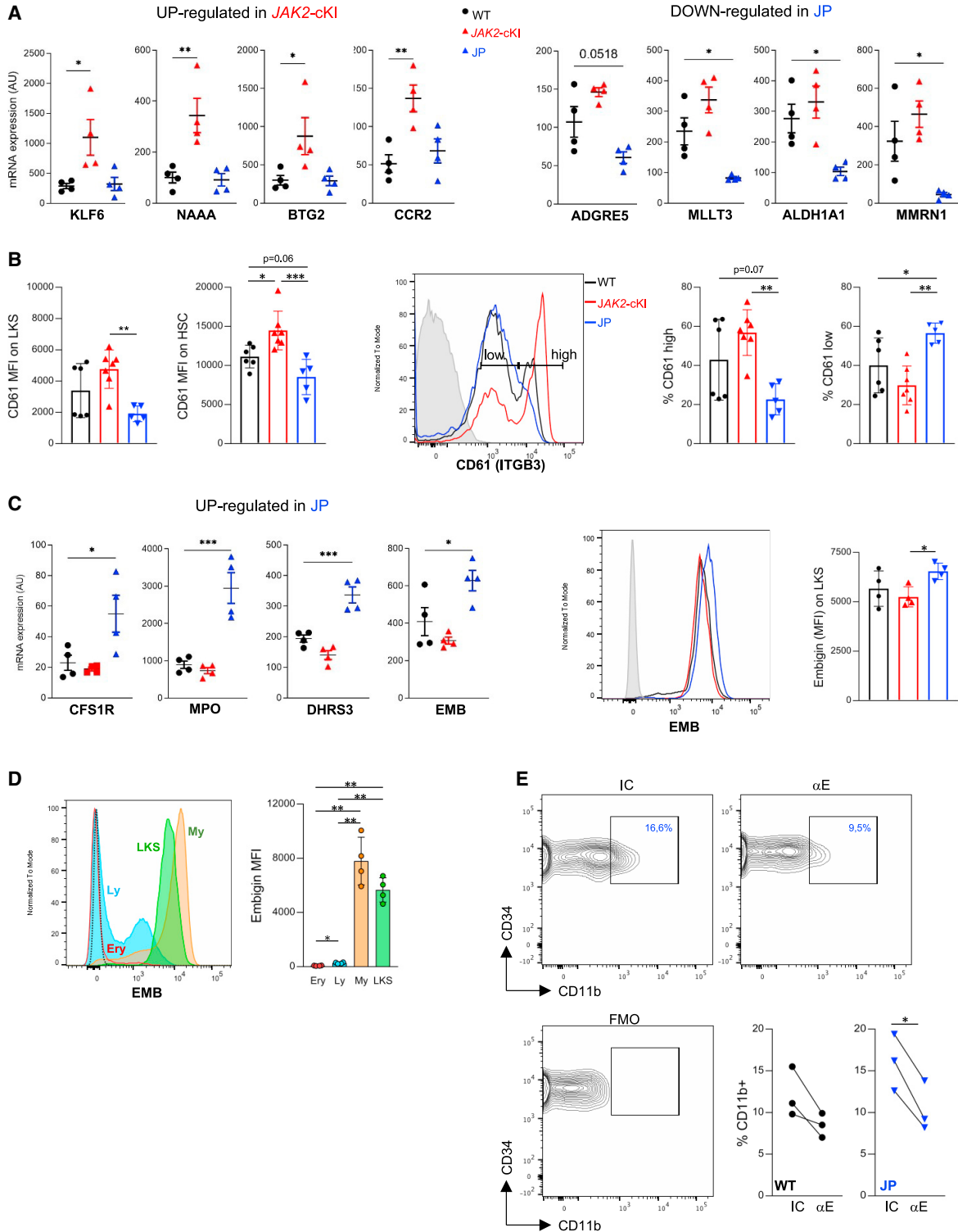
Figure 3. Validation of RNA-seq data

(A) Scatterplots showing real-time PCR data for the indicated genes expressed in arbitrary units (AU).

(B) FACS analysis showing CD61 expression in BM LKS and HSCs of pIpC-treated *JAK2*-cKI, JP, and WT mice. MFI, mean fluorescence intensity. Representative overlay histograms indicating CD61-high and -low gates are shown.

(legend continued on next page)

binding, platelet activation, and for previously published gene sets related to lipids. The same gene families and pathways were enriched in the list of genes downregulated in LKS from JP mice (Figure 2C, top), suggesting that their expression in LKS from MPN-affected mice is dependent on Pbx1.

Among genes DE in JP LKS compared with WT, we also found a significant overlap with the PBX1 signature (Figure 2D), indicating that at least part of the expression profile of the JP mice is the result of the absence of PBX1 per se, regardless of the JAK2 unregulated expression. Downregulated overlapping transcripts are mainly involved in calcium binding, HSC maintenance, cancer, and platelet development/function (Table S3), in line with our current experimental data; upregulated genes play roles in inflammation and in the innate immune system, as expected from *Pbx1*-cKO mice. However, most of the non-overlapping DE genes likely change their expression level as the result of the concomitant JAK2 constitutive expression and PBX1 absence. Of note, 32.5% of the genes downregulated in JP LKS (including *Pbx1*) are upregulated in MEP from a similar murine MPN model (Rao et al., 2019) (Figure 2E; Table S3), despite PBX1 not normally being expressed in MEP (Figure S4D), indicating that, by deleting *Pbx1* in HSCs constitutively expressing JAK2, a portion of the genes contributing to MPN acting in committed progenitors are already repressed in LKS. Sixteen percent of the overlapping genes are also overexpressed in human MPN (Table S3).

We validated part of RNA-seq data with real-time PCR or FACS analysis (Figures 3A–3C). We confirmed elevated expression of KLF6 (a transcriptional activator), of NAAA (involved in fatty acid metabolism), BTG2 (correlated to terminal differentiation), and CCR2 (a chemokine receptor) in *JAK2*-cKI LKS compared with WT (Figure 3A, left panels). Genes confirmed to be downregulated in JP LKS included MLLT3 and ALDH1A1 (HSC stemness), ADGRE5 (CD97, regulator of leukemia stem cell function), MMRN1, and ITGB3 (CD61,platelet function) (Figure 3A, right panels, and Figure 3B). Downregulation of CD61 was confirmed at the protein level on both LKS and HSCs (Figure 3B, left). FACS analysis revealed the presence of CD61 high- and CD61 low-expressing LKS cells (Figure 3B, right), with JP LKS showing a reduced proportion of the CD61-high fraction and a concomitant increase of the CD61-low fraction compared with *JAK2*-cKI and WT mice. Among genes upregulated in JP versus WT LKS, we tested CFS1R (CD115), MPO, DHRS3 (all normally expressed in myeloid cells) and Embigin (EMB; a cell adhesion molecule), which we also confirmed at the protein level (Figure 3C). Interestingly, FACS analysis of WT BM cells revealed an expression pattern that suggests EMB as a novel myeloid differentiation marker (Figure 3D). EMB was recently included among HSC regulators since its expression in the BM microenvironment promotes HSC homing (Silberstein et al., 2016); however, its function within HSPCs has not been dissected out. To gain insight into EMB's role within early progenitors, we sorted LKS cells and incubated them with an anti-EMB (αE)-blocking antibody (Ab) (Silberstein et al., 2016) in short-term culture. After 3 days, the proportion of cells that had acquired the CD11b myeloid marker was lower in cells treated with the αE Ab compared with isotype control (Figure 3E), suggesting that EMB downregulation prevents myeloid differentiation and that its overexpression in JP LKS, together with CFS1R and MPO, likely favors the myeloid lineage at the expenses of erythroid and MK lineages.

In conclusion, despite the blood pathology in MPN being mediated by differentiated cells, several molecular pathways are already deregulated in HSPCs. Transcriptional profiling data suggest that most of them are directly or indirectly under the control of PBX1. Our lists of DE genes provide a tool to select new therapeutic targets.

DISCUSSION

In this study, we demonstrate an essential role for PBX1 in determining the course of $JAK2^{V617F}$ MPN through the analysis of a mouse model of the disease. Our data indicate that, despite the mutation in *JAK2*, thrombocytosis and granulocytosis do not develop in the absence of PBX1, in accordance with the high level of expression of PBX1 in the progenitors of these lineages in normal conditions (Seita et al., 2012) and with the low number of platelets in *Pbx1*-cKO mice; importantly, we also show that erythrocytosis normalizes after a few weeks in JP mice. We confirm that PBX1 sustains the expression of transcriptional programs that control HSC maintenance and platelet development, and prevent myeloid skewing, all relevant for MPN

(C) Left: real-time PCR data for genes upregulated in JP mice. Right: EMB expression in BM LKS cells of *JAK2*-cKI, JP, and WT mice measured by FACS. (B–C) FACS histograms in gray: unstained control.

(D) EMB protein level in erythroid (Ery), lymphoid (Ly), myeloid (My) (all gated based on scatters), and LKS cells in the BM of WT mice; a representative FACS analysis is shown on the left (dotted line: unstained). (A–D) Ordinary one-way ANOVA.

(E) Percentage of cells expressing CD11b after 3 days of liquid culture of LKS cells treated with αE or isotype control (IC); representative FACS contour plots of a JP sample are shown; paired t test.

For all bar graphs, bars indicate mean ± SD. *, $p < 0.05$; **, $p < 0.01$, ***, $p < 0.001$.

onset, and we show that, in combination with mutated *JAK2*, PBX1 contributes to regulate signaling and metabolic pathways that are key for MPN and that are already active in primitive progenitors.

Conditional inactivation of PBX1 alone led to anemia, likely due to the known PBX1 role in preserving HSC functions and erythroid potential. Nevertheless, this property does not affect disease development during the first weeks after pIpC injection, underlying the prominent role of JAK2 signaling in promoting proliferation, survival, and differentiation of erythroid progenitors, despite PBX1 absence. However, our data suggest that, to fuel the disease, proper HSC functionality, including long-term self-renewal, must be maintained over time. Whether similar conclusions could be drawn by deleting other genes that maintain fitness of HSCs is worth investigating.

Since PBX1 must be expressed to sustain the disease, we propose that acting on PBX1, or on pathways downstream of it, might represent an option for a long-term cure of MPN, to complement the action of conventional therapies or of more recent treatments based on JAK inhibitors (Vannucchi and Harrison, 2017). Modulation of PBX1 activity by direct targeting or by targeting its downstream mediators might represent a novel therapeutic approach that likely hits MPN stem cells rather than the bulk of the disease. Small molecules targeting PBX1 have been developed and tested in cancer models (Morgan et al., 2012; Platais et al., 2018; Shen et al., 2018, 2019), and selective toxicity for neoplastic cells has been demonstrated *in vitro* (Liu et al., 2019); moreover, their therapeutic potential has been proposed for several types of tumors (Morgan et al., 2012). However, the high number of genes DE in JP LKS compared with WT, and the fact that some JP mice died likely of ineffective hematopoiesis, suggest some caution before considering PBX1 inhibition in patients. Our approach of genetic inactivation as a proof of principle is very different from a pharmacologic approach, which would include dosage studies and would likely not reach a total abrogation of PBX1 activity. However, we also encourage the development of alternative or complementary strategies that target some of the druggable genes and pathways described here that are subordinated to PBX1 in the presence of mutated *JAK2*. Moreover, whether PBX1 could represent a novel prognostic factor is worth investigating, with the aim of further stratifying these heterogeneous patients and personalizing their therapeutic approach.

EXPERIMENTAL PROCEDURES

Murine models

Mx1Cre⁺.JAK2^{+/V617F} and *Mx1Cre⁺.Pbx1^{fl/fl}* mice have been described (Crisafulli et al., 2019; Koss et al., 2012; Li et al., 2010); see also supplemental experimental procedures. Primers used for genotyping are listed in Table S4.

Induction of *JAK2^{V617F}* expression and *Pbx1* deletion

Three- to 6-week-old mice were treated with 10 mg/kg pIpC (high molecular weight, InvivoGen) by intraperitoneal injection (seven doses, every other day). A detailed description is provided in supplemental experimental procedures.

Histological and FACS analysis

A detailed description is provided in supplemental experimental procedures. Monoclonal antibodies are listed in Table S4.

Colony-forming unit assay

To evaluate erythropoietin (EPO) independency, colony-forming unit (CFU) assay was performed from BM cells using the CAMEO-4 Kit (Preferred Cell Systems) as previously described (Li et al., 2010), with and without 3 U/mL h-EPO (R&D). See also supplemental experimental procedures.

RNA-seq and bioinformatic analysis

Total RNA was extracted with Direct-zol RNA Microprep kit (Zymo Research) from 5×10^4 LKS sorted from the BM of pIpC-treated *JAK2*-cKI, JP, and WT control mice (3–4 biological replicates/group). A detailed description is provided in supplemental experimental procedures.

Statistics

For time course analysis of blood parameters, data were compared using ANOVA for repeated measures when considering the entire curve, or with one-way ANOVA with *post hoc* Tukey's multiple comparison test when comparing individual time points. For all other multiple comparisons, Kruskal-Wallis test with Dunn's multiple comparisons test was used if normality test was not passed, or ordinary one-way ANOVA if data followed a normal distribution. $p < 0.05$ was considered statistically significant (* and #$p < 0.05$, ** and ##$p < 0.01$, *** and ###$p < 0.001$, ****$p < 0.0001$). Analyses were performed with GraphPad Prism (GraphPad Software) or with Stata15 (StataCorp LLC).

Data and code availability

The accession number for the RNA-seq data reported in this paper is GEO: GSE153482.

SUPPLEMENTAL INFORMATION

Supplemental information can be found online at https://doi.org/10.1016/j.stemcr.2021.09.016.

AUTHOR CONTRIBUTIONS

CONFLICT OF INTERESTS

ACKNOWLEDGMENTS

REFERENCES

Akada, H., Akada, S., Hutchison, R.E., Sakamoto, K., Wagner, K.U., and Mohi, G. (2014). Critical role of Jak2 in the maintenance and function of adult hematopoietic stem cells. Stem Cells *32*, 1878–1889.

Berkofsky-Fessler, W., Buzzai, M., Kim, M.K., Fruchtman, S., Najfeld, V., Min, D.J., Costa, F.F., Bischof, J.M., Soares, M.B., McConnell, M.J., et al. (2010). Transcriptional profiling of polycythemia vera identifies gene expression patterns both dependent and independent from the action of JAK2V617F. Clin. Cancer Res. *16*, 4339–4352.

Crisafulli, L., Muggeo, S., Uva, P., Wang, Y., Iwasaki, M., Locatelli, S., Anselmo, A., Colombo, F.S., Carlo-Stella, C., Cleary, M.L., et al. (2019). MicroRNA-127-3p controls murine hematopoietic stem cell maintenance by limiting differentiation. Haematologica *104*, 1744–1755.

Ficara, F., Crisafulli, L., Lin, C., Iwasaki, M., Smith, K.S., Zammataro, L., and Cleary, M.L. (2013). Pbx1 restrains myeloid maturation while preserving lymphoid potential in hematopoietic progenitors. J. Cell Sci. *126*, 3181–3191.

Ficara, F., Murphy, M.J., Lin, M., and Cleary, M.L. (2008). Pbx1 regulates self-renewal of long-term hematopoietic stem cells by maintaining their quiescence. Cell Stem Cell *2*, 484–496.

Guglielmelli, P., Zini, R., Bogani, C., Salati, S., Pancrazzi, A., Bianchi, E., Mannelli, F., Ferrari, S., Le Bousse-Kerdiles, M.C., Bosi, A., et al. (2007). Molecular profiling of CD34+ cells in idiopathic myelofibrosis identifies a set of disease-associated genes and reveals the clinical significance of Wilms' tumor gene 1 (WT1). Stem Cells *25*, 165–173.

Jung, J.G., Shih, I.M., Park, J.T., Gerry, E., Kim, T.H., Ayhan, A., Handschuh, K., Davidson, B., Fader, A.N., Selleri, L., et al. (2016). Ovarian cancer chemoresistance relies on the stem cell reprogramming factor PBX1. Cancer Res. *76*, 6351–6361.

Koss, M., Bolze, A., Brendolan, A., Saggese, M., Capellini, T.D., Bojilova, E., Boisson, B., Prall, O.W., Elliott, D.A., Solloway, M., et al. (2012). Congenital asplenia in mice and humans with mutations in a Pbx/Nkx2-5/p15 module. Dev. Cell *22*, 913–926.

Li, J., Spensberger, D., Ahn, J.S., Anand, S., Beer, P.A., Ghevaert, C., Chen, E., Forrai, A., Scott, L.M., Ferreira, R., et al. (2010). JAK2 V617F impairs hematopoietic stem cell function in a conditional knock-in mouse model of JAK2 V617F-positive essential thrombocythemia. Blood *116*, 1528–1538.

Liu, Y., Xu, X., Lin, P., He, Y., Zhang, Y., Cao, B., Zhang, Z., Sethi, G., Liu, J., Zhou, X., et al. (2019). Inhibition of the deubiquitinase USP9x induces pre-B cell homeobox 1 (PBX1) degradation and thereby stimulates prostate cancer cell apoptosis. J. Biol. Chem. *294*, 4572–4582.

Longobardi, E., Penkov, D., Mateos, D., De Florian, G., Torres, M., and Blasi, F. (2014). Biochemistry of the tale transcription factors PREP, MEIS, and PBX in vertebrates. Dev. Dyn. *243*, 59–75.

Mead, A.J., and Mullally, A. (2017). Myeloproliferative neoplasm stem cells. Blood *129*, 1607–1616.

Moens, C.B., and Selleri, L. (2006). Hox cofactors in vertebrate development. Dev. Biol. *291*, 193–206.

Morgan, R., Boxall, A., Harrington, K.J., Simpson, G.R., Gillett, C., Michael, A., and Pandha, H.S. (2012). Targeting the HOX/PBX dimer in breast cancer. Breast Cancer Res. Treat. *136*, 389–398.

Nangalia, J., and Green, A.R. (2017). Myeloproliferative neoplasms: from origins to outcomes. Blood *130*, 2475–2483.

Nourse, J., Mellentin, J.D., Galili, N., Wilkinson, J., Stanbridge, E., Smith, S.D., and Cleary, M.L. (1990). Chromosomal translocation t(1;19) results in synthesis of a homeobox fusion mRNA that codes for a potential chimeric transcription factor. Cell *60*, 535–545.

Platais, C., Radhakrishnan, R., Niklander Ebensperger, S., Morgan, R., Lambert, D.W., and Hunter, K.D. (2018). Targeting HOX-PBX interactions causes death in oral potentially malignant and squamous carcinoma cells but not normal oral keratinocytes. BMC Cancer *18*, 723.

Rampal, R., Al-Shahrour, F., Abdel-Wahab, O., Patel, J.P., Brunel, J.P., Mermel, C.H., Bass, A.J., Pretz, J., Ahn, J., Hricik, T., et al. (2014). Integrated genomic analysis illustrates the central role of JAK-STAT pathway activation in myeloproliferative neoplasm pathogenesis. Blood *123*, e123–e133.

Rao, T.N., Hansen, N., Hilfiker, J., Rai, S., Majewska, J.M., Lekovic, D., Gezer, D., Andina, N., Galli, S., Cassel, T., et al. (2019). JAK2-mutant hematopoietic cells display metabolic alterations that can be targeted to treat myeloproliferative neoplasms. Blood *134*, 1832–1846.

Rice, K.L., Lin, X., Wolniak, K., Ebert, B.L., Berkofsky-Fessler, W., Buzzai, M., Sun, Y., Xi, C., Elkin, P., Levine, R., et al. (2011). Analysis of genomic aberrations and gene expression profiling identifies novel lesions and pathways in myeloproliferative neoplasms. Blood Cancer J. *1*, e40.

Seita, J., Sahoo, D., Rossi, D.J., Bhattacharya, D., Serwold, T., Inlay, M.A., Ehrlich, L.I., Fathman, J.W., Dill, D.L., and Weissman, I.L. (2012). Gene Expression Commons: an open platform for absolute gene expression profiling. PLoS One *7*, e40321.

Shen, A.Y., Jung, J., Rahmanto, Y.S., Selleri, L., Shih, I.-M., Chuang, C.M., and Wang, T.-L. (2018). A novel small-molecule compound targeting PBX1-DNA interaction impedes cancer cell survival and carboplatin resistance. In Proceedings of the American Association for Cancer Research Annual Meeting 2018, 78 (AACR), Abstract nr: 1966.

Shen, L.Y., Zhou, T., Du, Y.B., Shi, Q., and Chen, K.N. (2019). Targeting HOX/PBX dimer formation as a potential therapeutic option in esophageal squamous cell carcinoma. Cancer Sci. *110*, 1735–1745.

Shepherd, M.S., Li, J., Wilson, N.K., Oedekoven, C.A., Li, J., Belmonte, M., Fink, J., Prick, J.C.M., Pask, D.C., Hamilton, T.L., et al. (2018). Single-cell approaches identify the molecular network driving malignant hematopoietic stem cell self-renewal. Blood *132*, 791–803.

Silberstein, L., Goncalves, K.A., Kharchenko, P.V., Turcotte, R., Kfoury, Y., Mercier, F., Baryawno, N., Severe, N., Bachand, J., Spencer, J.A., et al. (2016). Proximity-based differential single-cell analysis of the niche to identify stem/progenitor cell regulators. Cell Stem Cell *19*, 530–543.

Tefferi, A. (2016). Myeloproliferative neoplasms: a decade of discoveries and treatment advances. Am. J. Hematol. *91*, 50–58.

Vannucchi, A.M., and Harrison, C.N. (2017). Emerging treatments for classical myeloproliferative neoplasms. Blood *129*, 693–703.

Wei, X., Yu, L., and Li, Y. (2018). PBX1 promotes the cell proliferation via JAK2/STAT3 signaling in clear cell renal carcinoma. Biochem. Biophys. Res. Commun. *500*, 650–657.